TSUNAMI EVACUATION MODEL IN THE PANIMBANG SUBDISTRICT, BANTEN PROVINCE, INDONESIA: GIS- AND AGENT-BASED MODELING APPROACHES

Dini PURBANI[1], Marza Ihsan MARZUKI[2], Budianto ONTOWIRJO[3], Farhan Makarim ZEIN[4], Didik Wahju Hendro TJAHJO[1], Sri Endah PURNAMANINGTYAS[1] Rudhy AKHWADY[1], Amran Ronny SYAM[1], Arip RAHMAN[1], Yayuk SUGIANTI[1] Safar DODY[5], Adriani Sri NASTITI[1], Andri WARSA[1], Lismining Pujiyani ASTUTI[1] YOSMANIAR[6], Tutik KADARINI[7], Tri Heru PRIHADI[7] and Ulung Jantama WISHA[5,8*]

DOI: 10.21163/GT_2023.182.10

ABSTRACT:
This study examines the agent behavior during a complex tsunami process to reach designated shelters based on the agent-based modeling approach. A GIS-based tsunami inundation modeling is employed considering the land slope and surface roughness coefficient to estimate the tsunami height loss. This model becomes the basis for determining the service area within the study site. Five shelter candidates are assessed using agent-based modeling simulated in the NetLogo, implementing the 50 minutes ETA and 9 meters tsunami run-up propagation for four population age classifications. Overall, the Panimbang coastal area is categorized as a high vulnerability to tsunamis (14.68% of the total area), where the run-up propagation is extended due to the tsunami invading rivers, thereby increasing the risk toward local society. Of particular concern, two proposed shelters (SA1 and SA5) exceed the capacity by 12.43% and 59.44% of their maximum capacity, respectively. Of 9,640 agents (people) simulated, 77.7% are evacuated, and 22.3% fail to reach the shelters, with a majority of the adult category. A sufficiently high casualty number is due to a "bottleneck" in the overlapping service areas. However, reconsidering the overcapacity TES with some additional shelters in the surrounding area is recommended.

Key-words: *evacuation service area, NetLogo, volcanic tsunami, spatial analysis, bottleneck conditions*

1. INTRODUCTION

The strategic position of the Indonesian archipelago is always linked to the potency of geological hazards and disasters. One is the volcanic tsunami threat in the Sunda Strait. On 22 December 2018, a giant tsunami occurred, affected by a lateral collapse on the southwest flank of Anak Krakatau (AK) (Grilli et al., 2019; Muhari et al., 2019). According to BNPB (National Disaster Management Authority) in 2019, casualties resulted from that event 437 people were killed, more than 7200 injured,

[1]*Research Center for Conservation of Marine and Inland Water Resources, National Research and Innovation Agency (BRIN), Cibinong, Indonesia, dini017@brin.go.id, didi029@brin.go.id, srie005@brin.go.id, rudh002@brin.go.id, amra002@brin.go.id, arip004@brin.go.id, yayu003@brin.go.id, adri005@brin.go.id, andr055@brin.go.id, lism003@brin.go.id.*
[2]*Research Center for Artificial Intellegence and Cyber Security, National Research and Innovation Agency (BRIN), Bandung, Indonesia, marz002@brin.go.id .*
[3]*Civil Engineering Department, Faculty of Engineering and Computer Sciences, Bakrie University, Jakarta, Indonesia, budianto.ontowirjo@barkie.ac.id*
[4]*Department of Geography, Faculty Mathematics and Natural Sciences, University of Indonesia, Depok, Indonesia, farhan.makarim@ui.ac.id*
[5]*Research Center for Oceanography, National Research and Innovation Agency (BRIN), Jakarta, Indonesia, safa001@brin.go.id , ulun002@brin.go.id *.*
[6]*Research Center for Marine and Land Bioindustry, National Research and Innovation Agency (BRIN), North Lombok, Indonesia, yosm003@brin.go.id .*
[7] *Fisheries Research Center, National Research and Innovation Agency (BRIN), Cibinong, Indonesia, tuti006@brin.go.id , trih016@brin.go.id .*
[8]*Department of Physics and Earth Sciences, Graduat School of Engineering and Science, University of the Ryukyus, Nishihara, Japan.*

and 46,646 people lost their homes. The volcanic eruption-induced tsunami is generally evoked by an underwater explosion or airwave generated by the blast. These pyroclastic flows entered the sea, causing the collapse of an underwater caldera, subaerial and submarine failure (Paris et al., 2014).

In the Sunda Strait, a Megathrust subduction zone has previously been observed (Kurniawan et al., 2021). On the other hand, the AK Volcano makes this area more prone to tsunamis, both caused by earthquakes and volcanic eruptions. From year 416 to 2018, the immense strength of a tectonic earthquake was reported on 24 August 1757 in the Java Sea (northeast of the Sunda Strait) with a magnitude of 7.5 and 16 December 1963 in Banten with a magnitude of 6.5 (Triyono et al., 2019).

Since several extraordinary earthquake and tsunami events had occurred in western Sumatra and the south of Java, these regions have become more vulnerable. On the other hand, due to the prone area, the Agency for Assessment and Application of Technology (BPPT) has designed and created a system for the Tsunami Early Warning System (TEWS), which has been deployed in places with high potency of tsunami events (Priohutomo et al., 2022). Locations with frequent occurrences of the tsunami are southern Sumatra, southern Java, and the waters of Maluku and Halmahera. Several systems have been initiated based on sudden sea-level changes in the West Sumatra, Aceh, Pangandaran, and Sunda Straits, such as the Inexpensive Device for Sea Level (IDSL) monitoring (Husrin et al., 2021). In addition to disaster mitigation, evacuation routes in the prone areas do not exist, and in some cases, it does not show the proper and safe evacuation routes. These issues can be found in several prone areas in the surrounding Sunda Strait.

Tsunami preparedness strategies in vulnerable areas are crucial to initiate where information about evacuation routes is not entirely established. One is the Panimbang Subdistrict, located at the westernmost tip of Pandeglang Regency, Banten Province, directly facing the Sunda Strait (Sari & Soesilo, 2020). Panimbang Subdistrict has become an area of significance because of an exclusive tourism development where Tanjung Lesung has become the point of the developing economy (Mulyadi & Nur, 2018). Furthermore, even though a natural green belt (mangrove conservation area) is situated in Panimbang Subdistrict, the other land uses of the coastal zone for settlement and tourism could increase the risk of tsunami or other disasters. Therefore, information regarding this area's hazardous seismic events and evacuation routes is crucial and could be a basis for future developments.

Concerning the evacuation routes, since, to date, there are no evacuation shelters and signs established in the Panimbang Subdistrict, an evaluation of the transportation lane network and agent-based modeling (ABM) is essential to be conducted in this region. This approach was previously introduced by Mas et al. (2012), where every individual (agent) is a part of a system modeled as an entity of autonomous decision-makers, and every agent obeys specific rules as their roles within the system (Pizarro et al., 2022). This method is often used and simulated in tsunami-impacted areas to determine any possibilities when a tsunami occurs (Jacob et al., 2014; Kim et al., 2022; Mas et al., 2012; Mostafizi et al., 2017; Usman et al., 2017; Wafda et al., 2013; Wang & Jia, 2021, 2022). Since agent-based modeling is well-known among scholars and could concisely simulate the evacuation routes of any conditions during tsunami run-up, we used this method for a case study in Panimbang Subdistrict with some modifications based on local environmental states.

We report herein the result of ABM combined with several GIS-based techniques to map the evacuation routes, shelter capacity, and any possibility of agent behavior during tsunami events applied in the Panimbang Subdistrict, considering the social and population data. A few studies have reported tsunami inundation and ABM modeling in the study area. Farahdita & Siagian (2020) assessed the tsunami inundation and the land use change due to the tsunami in the coastal area of Panimbang Subdistrict using Sentinel-2 images, DEM, and unsupervised classification methods.

On the other hand, Lee et al. (2022), modeled the tsunami hazard in the Panimbang Subdistrict using the ABM approach, where they considered several transportation modes and existing physical buildings as shelters. Spatial-based estimation of the tsunami inundation area with several scenarios of tsunami height has never been done to date. Moreover, since the number of transportation modes in the Panimbang could not be precisely determined, the ABM simulation considering travel time on foot as the worst-case during a tsunami event is also essential to examine. As such, these aspects

should be investigated. Therefore, this study aimed to evaluate horizontal evacuation zones based on the pattern of agent's mobility during a scenario of tsunami event in the Panimbang Subdistrict. This study is also expected to be a basis for future decision-making and development of the Pandeglang Regency, especially for early mitigation and preparing the proper evacuation routes and tsunami shelters.

2. STUDY AREA

As previously introduced, the study area is situated in the Panimbang Subdistrict, Pandeglang Regency, Banten Province, Indonesia. Based on overlayed DEM (Digital Elevation Model) and SRTM (Shuttle Radar Topography Mission) data, the coastal morphology of the Panimbang Subdistrict is a flat beach with a slope ranging from <2.5 to 5 m above sea level (**Fig. 1**). The total area of the Panimbang Subdistrict is approximately 97.75 km^2 (3.56% of the total area of the Pandeglang Regency). It is bordered by Sukaresmi Subdistrict in the north, Angsana Subdistrict in the east, Cigeulis and Sobang Subdistricts in the south, and the Sunda Strait in the west. In particular, the total area of Citeurep and Mekarsari, the area of interest in this study, is approximately 17.1 and 23.1 km^2, respectively (about 17.4 and 23.6% out of the Panimbang Subdistrict). Concerning the total population, the number of villagers in Citeureup and Mekarsari is about 9,174 and 11,189, respectively.

The tsunami event in 2018 induced by the Krakatoa volcano significantly impacted the environment in the locality, specifically resulting in a change in land use, whereby the prone area is situated between 50-300 meters from the coastline (Farahdita & Siagian, 2020). The green belt declined by 205.714 ha, and the settlement area decreased by 25.17 ha. The farming area and the shoreline pattern of rivers and estuaries have also been altered. Many empty and open land areas show how powerful the volcanic tsunami event was in the past (Pradjoko et al., 2015).

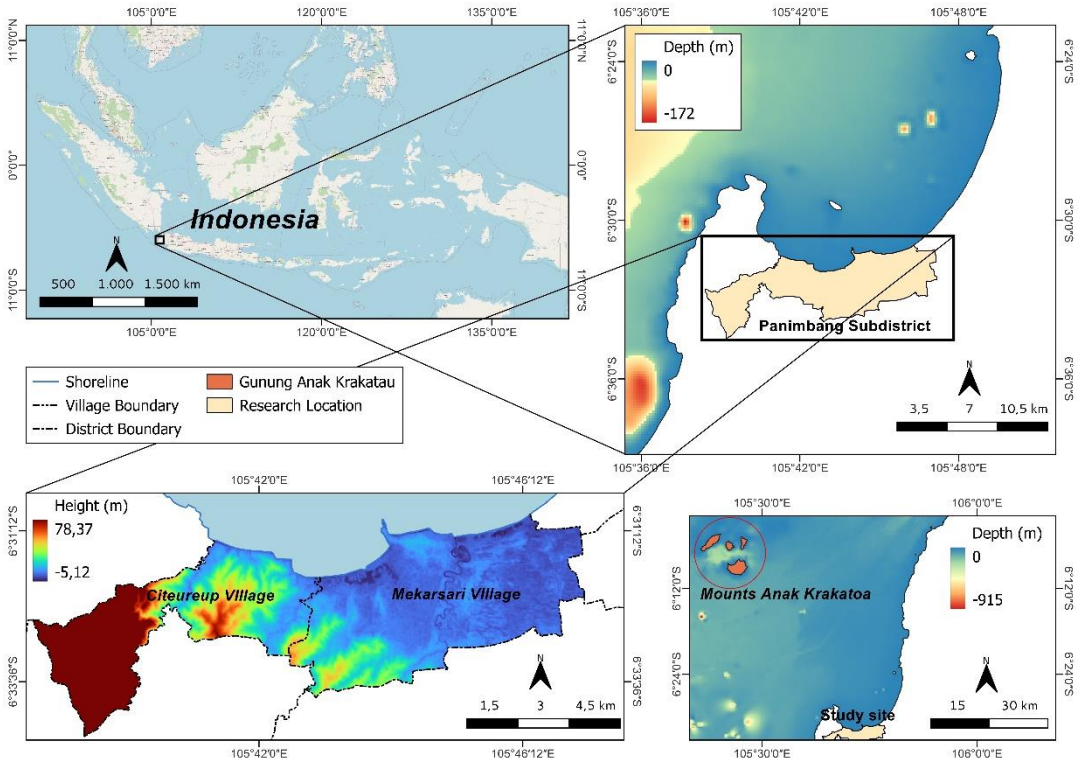

Fig. 1. The assessed area covering Citeureup and Mekarsari Villages in the Panimbang Subdistrict.

3. DATA AND METHODS

3.1. Spatial-based tsunami inundation modeling

Berryman (Berryman, 2006) previously established a numerical modeling approach, which was used in this study. This method calculates the tsunami height loss for every one meter of inundation distance, considering the slope and surface roughness as follows:

$$H_l = \left(\frac{167sr^2}{H_0^{1/3}}\right) + 5\sin S \quad (1)$$

where:

H_l= the loss in wave height per meter of inundation slope (m)

sr= surface roughness coefficient

H_0= initial wave height in the coastline (m)

S= land surface slope (degree)

The data used to simulate tsunami inundation model consist of Panimbang's administration data, DEM, and Sentinel-2 imagery (**Table 1**). The DEM data were resampled to equalize the spatial resolution between DEM and Sentinel-2 imagery (Danardono et al., 2023). The resampled data were then processed using the slope generation technique to produce the land surface slope of the study area (Marzuki et al., 2021). The Sentinel-2 image used in this study was acquired on August 12th, 2021, with the tile of T48MWT. Sentinel-2 has 13 spectral bands: four bands with a 10-meter resolution, six bands with a 20-meter resolution, and three bands with a 60-meter resolution (Phiri et al., 2020). This image's orbital coverage area is approximately 290 km. In this simulation, we only used four bands: band 2 (blue), 3 (green), 4 (red), and 8 (Near-Infrared/NIR). These four bands were classified by applying Spectral Angle Mapping with 94% accuracy, in which the classification used consisted of developed areas, rice fields, forests, and water bodies (Pesaresi et al., 2016).

Table 1.

The primary data used in the tsunami inundation modeling.

Data	Type	Resolution	Source
Administration data	Polygon	-	GADM (Global Administrative Areas)
DEM (1109-24, 1109-23, 1109-52, 1109-51)	Raster	8.5 m	DEMNAS (National Digital Elevation Model for Coastal Application)
Sentinel-2 Imagery	Raster	10 m	ESA (European Space Agency)

The classification results were then reclassified based on the concept of empirical multidimensional histogram to produce the surface roughness coefficient (Pesaresi et al., 2016) (**Table 2**). The value of surface roughness was considered to estimate the wave height attenuation. According to Borrero et al. (2020), the expected tsunami run-up in the northern tip of Tanjung Lesung Peninsula approximately ranges from 7 to 13.5 meters. However, this study simulated the 9-meter run-up height of a volcanic-induced tsunami in the Panimbang Subdistrict. Moreover, simulations with variations in tsunami run-up heights (7 and 13.5 meters) were also performed for different tsunami run-ups in the Panimbang coastal zone. The tsunami run-up combined with water channels flowing in the rough topography regimes, such as dunes, coastal vegetation, buildings, erratic topography profile, rivers, and other land covers on the surface, is the most significant parameter to estimate the inundated area (Berryman, 2006).

After gaining the tsunami height loss, a cost distance analysis was employed to estimate the cost distance of a one-meter tsunami height loss, where the height loss was used to monitor the maximum inundated area. The result of cost distance was then used for processing fuzzy membership and index for creating classification levels within a category or class (Berryman, 2006; Zaman et al., 2014). In this case, the impacted region was classified into highly vulnerable (3), moderately vulnerable (2), and lowly vulnerable (1).

Table 2.
The value of surface roughness for every land cover type, modified from (Berryman, 2006).

Land cover	Surface roughness coefficient
Water body	0.007
Swamp	0.015
Pond	0.007
Embankment	0.010
Sands/dunes	0.018
Bushes	0.040
Meadow	0.020
Forest	0.070
Plantation	0.035
Moore/Field	0.030
Rice field	0.020
Agriculture area	0.025
Settlement/developed area	0.050
Mangrove forest	0.060

3.2. Deciding TES in the Panimbang Subdistrict

A genuine horizontal temporary evacuation shelter (TES) was assessed in this study. A horizontal shelter is a public area that area-wise could accommodate evacuees (Mück & Post, 2008). Several parameters were considered to decide the shelter criteria relying on the local administrative data, such as road networks, building existence, demography, overlaid using tsunami vulnerability map. The proposed horizontal TES should be situated at a higher elevation (above the tsunami-inundated area), on a less than 20^{o} slope and flat terrain, with easy access to the main road (secondary road), in the surrounding dense area (settlement), in the area more than 10,000 m^{2}, located in an open area 200 meters off the coastline (Lakshay et al., 2016; Mück & Post, 2008; Taubenböck et al., 2013).

The road network, width, and conditions in the study area were surveyed using OpenStreetMap application and validated using a high-resolution Google Earth image. The open area was determined by applying Google Street View with a 360^{o} angle to analyze the land use of each proposed shelter (Li et al., 2017). These data are fairly accurate since it is recorded within on average 6 meters distance from the object, with approximately 80% overlap of moving objects between two datasets (Brovelli and Zambogini, 2018).

3.3. Shelter assessment based on Agent-Based Modeling

The proposed TES was assessed using an agent-based model (ABM). This modeling technique is based on agents and simulates evacuation of a natural hazard (Pizarro et al., 2022). The model processing is based on the agent behavior where the evacuee (agent) is the entity to decide whether to evacuate or not during a disaster event. The evacuation modeling is built using a NetLogo application, multi-agent programming language, and environmental modeling for a complex phenomenon (Mas et al., 2012).

Agents will move toward the closest proposed shelters via the most accessible way. Therefore, the maximum population capacity that each shelter could service was estimated using a service area analysis. This analysis is based on a network analysis method, considering the road facility, dense settlement area, travel speed and time, and travel distance (Kuller et al., 2019). The slowest speed belongs to the elders' cohort, with 0.93 m/s (Mas et al., 2012). The time travel of tsunami wave inundation was 40 minutes, estimated by the last report of volcanic-based tsunami modeling in the Sunda Strait (Dogan et al., 2021).

After gaining each shelter's service area, the building amount and road networks in the surrounding location was calculated and extracted from OpenStreetMap data. Concerning four people in a building, every building was multiplied by four to obtain the maximum population capacity that

shelters could service. This consideration was based on the Central Agency of Statistics data in 2019, whereby the average amount of family members in one house/building in the study area was 3.9≈4. However, the actual field data could be more than that. On the other hand, the population was classified into four classes: kids (0−9 years old), teens (10−19 years old), adults (20−64 years old), and elders (>64 years old). In addition to the number of agents, we considered the maximum population capacity that could be serviced by all shelters as follows:

$$Ta = 4 \times Tb \times Cp \quad (2)$$

where:

Ta = The total of agent
Tb = The total of calculated buildings
Cp = The age class percentage

The amount of agent was used for further processing in the NetLogo application applying a modified code previously established by Mas et al. (2015). The considered parameters were ETA (estimated time of arrival, about 50 minutes) and the number of agents according to the age classification. The workflow of this study is shown in **Fig. 2**.

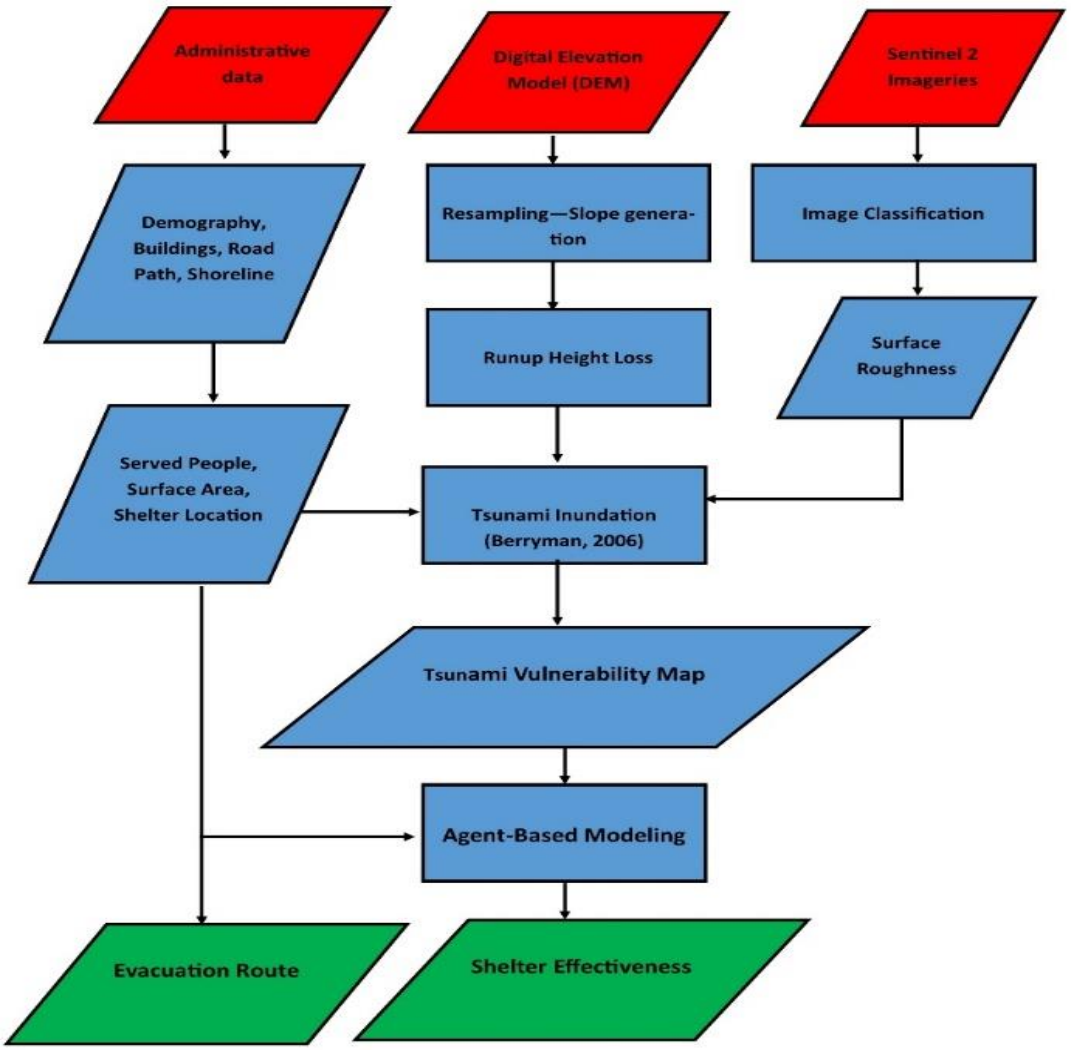

Fig. 2. The workflow of this study.

4. RESULTS AND DISCUSSIONS

4.1. The vulnerability map of tsunami in the Panimbang Subdistrict

Panimbang Subdistrict consists of two villages, Citereup and Mekarsari, situated on the coastline of Sunda Strait. **Fig. 3A** shows the vulnerable areas prone to tsunamis based on inundation modeling. Overall, the vulnerable coastal area is only 14.68% of the total area of the Panimbang Subdistrict. The most impacted area by the tsunami is observed in the Mekarsari Village, with 7.89% highly vulnerable area. The remnant classifications are moderately vulnerable (2.59%) and lowly vulnerable (1.86%) (**Fig. 3D**). By contrast, in the Citeureup Village, the area categorized as high vulnerability only covers 2.06%, with a small portion of moderate-low categories (less than 1%) (**Fig. 3C**). Since tsunami inundation modeling relies on land topography and elevation, the more declivous the slope, the more vulnerable to tsunami (Berryman, 2006). In this case, Mekarsari Village is situated on the more declivous slope ranging between 15 to 25°, while the Citeureup is situated in a higher elevation with a slope reaching 30°.

The vulnerable area to the tsunami in the Panimbang Subdistrict encompasses many types of land use (**Fig. 3B**). Based on GIS-based analysis, the volcanic-induced tsunami inundates approximately 190.384 ha (49.57%) of agricultural areas. Moreover, the other impacted areas are settlements (built areas) with a coverage of 87.23 ha (21.93%), 71.37 ha (18.84%) of forest, and 37.04 ha (9.65%) of water bodies. Concerning the built area, the number of impacted buildings is approximately 519 in Citeureup and 753 in Mekarsari, respectively, which are mainly located in the highly vulnerable area (26% out of 36.64% of impacted buildings). Even though the inundated area is more extensive in Mekarsari than in Citeureup, the number of impacted buildings is higher in Citeureup.

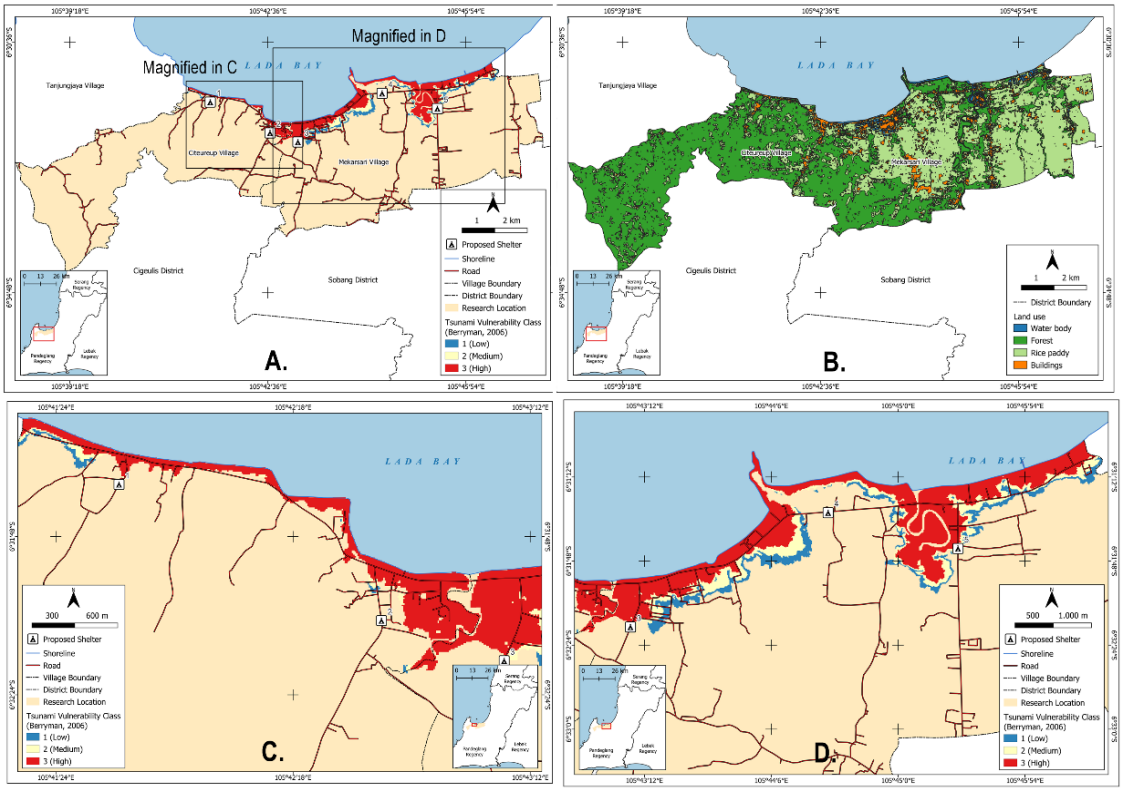

Fig. 3. The vulnerable coastal area based on tsunami inundation modeling with 9-m tsunami run-up height (A), the land use of Panimbang Subdistrict (B), the magnified inundated area in the Citeureup Village (C), and the magnified inundated area in the Mekarsari Village (D).

The most extensive inundation zone is observed in the surrounding estuaries and rivers (**Fig. 3**). However, the area with a higher surface roughness coefficient could significantly reduce tsunami propagation. According to Yamanaka & Shimozono (2022) and Yeh et al. (2012), a tsunami invading a river channel could cause it to overflow. By contrast, the built-up areas could significantly decrease the total amount of tsunami inundation for the sites behind them, even though at some points, the building and coastal structures may increase the tsunami height immediately in other areas nearby (Bricker et al., 2015). Concerning the land use of Panimbang Regency, the dense population and buildings are situated in the coastal zone and rivers (highly vulnerable to tsunamis). Therefore, mitigation efforts to minimize the impact of tsunami hazards are crucial to be initiated by local and central government since there is no protection, shelter, or proper evacuation route in the Panimbang Regency.

The coastal vulnerability maps based on scenarios of 7-meter and 13.5-meter run-up heights are shown in **Fig. 4**.

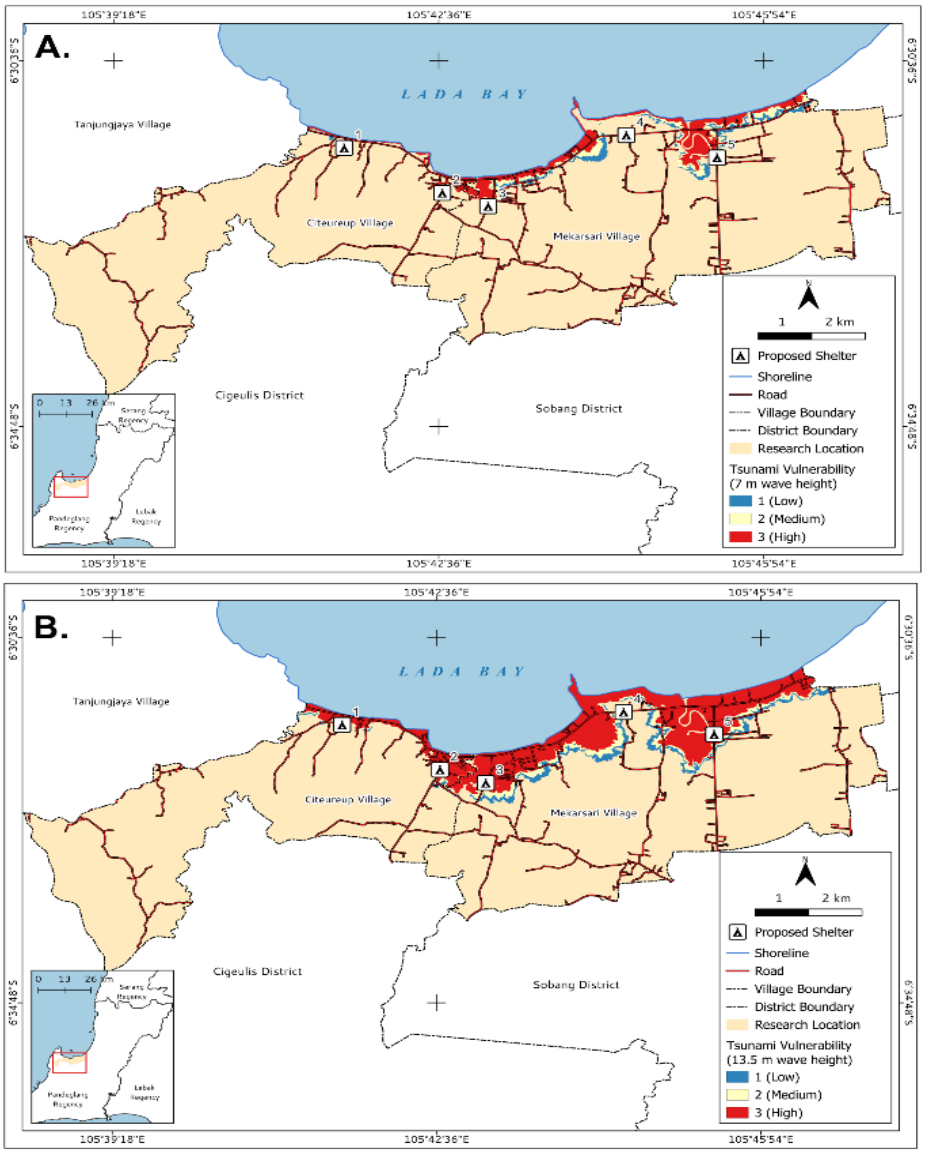

Fig. 4. The vulnerable coastal area based on tsunami inundation modeling with run-up height of 7 meters (A) and 13.5 meters (B).

Overall, compared to the result of the 9-meter tsunami run-up height, the lower run-up decreases the amount of the impacted areas over the Panimbang Subdistrict by less than 50%. On the other hand, the higher run-up height (13.5 m in maximum) will significantly increase the inundated area by more than 50%.

By reducing the run-up height set up by about 2 meters, the low vulnerability area decreases by about 42,800 m^2 (8.03%), the moderate vulnerability area decreases by about 79,300 m^2 (10.61%), and the highly vulnerable area reduces by approximately 43.34% (**Fig. 4A**). On the other hand, compared to the total area of the Panimbang Subdistrict, the low, moderate, and high vulnerability areas cover about 1.13%, 1.59%, and 5.48%, respectively.

Another simulation with a 13.5-m run-up height is shown in **Fig. 4B**. Based on the spatial calculation, with the increase of run-up height of about 4.5 meters, the inundated area categorized as highly vulnerable covers 11.03% of the total area of Panimbang. On the other hand, the regions with moderate and low vulnerability only expand by less than 2%. Compared to the inundation area in the 9-meter run-up height simulation, the coverage area increases by 29.12%, 14.23%, and 50.35% for low, moderate, and high vulnerability categories, respectively.

4.2. Proposed horizontal TES in the Panimbang Subdistrict

Based on the tsunami inundation area, five prospective horizontal shelters throughout the Panimbang Subdistrict were proposed in this study. Overall, the proposed shelters meet the requirement for an evacuation area, consisting of one shelter in Citeureup, three shelters in Mekarsari, and another in between. Except for shelters SA2 and SA3, the other shelters could be accessed using vehicles due to more extensive access (around 10 meters in width). Furthermore, all shelters were positioned in the declivous area with a slope ranging from 0−10° and land elevation of around 10−15 meters (**Table 3**).

Table 3.

The information of tsunami shelters in the Panimbang Subdistrict.

Shelter Code	Longitude (°East)	Latitude (°South)	Location	The road width (m)	Materials	Elevation (m)	Slope (°)	The number of buildings	Capacity (people)	The area of shelter (ha)
SA1	105.6939	6.5433	Citeureup Village	10	Paving blocks	14.39	10.11	137	548	308.7
SA2	105.7106	6.5353	(Citeureup-Mekarsari)	7	Asphalt	12.12	4.25	753	3012	748.33
SA3	105.7184	6.5378	Mekarsari Village	1.5	Concrete	9.58	4.10	764	3056	597.29
SA4	105.7417	6.5242	Mekarsari Village	2.5	Soil and rocks	11.39	2.48	396	1584	455.47
SA5	105.7571	6.5285	Mekarsari Village	10	Concrete	9.34	0.89	360	1440	552.58

Shelter 1 (SA1) is positioned approximately 230 meters from the coastline, 60 meters from the low vulnerability area, and about 2.3 km from shelter 2 (SA2) (**Fig. 5A**). This shelter is situated in a resort with a 10 meters road width and paving block materials. Land use-wise, this area is categorized as an open space with a total area of about 308.7 ha. This area is smaller than the other shelters that could only service 548 people with a density of one person per hectare.

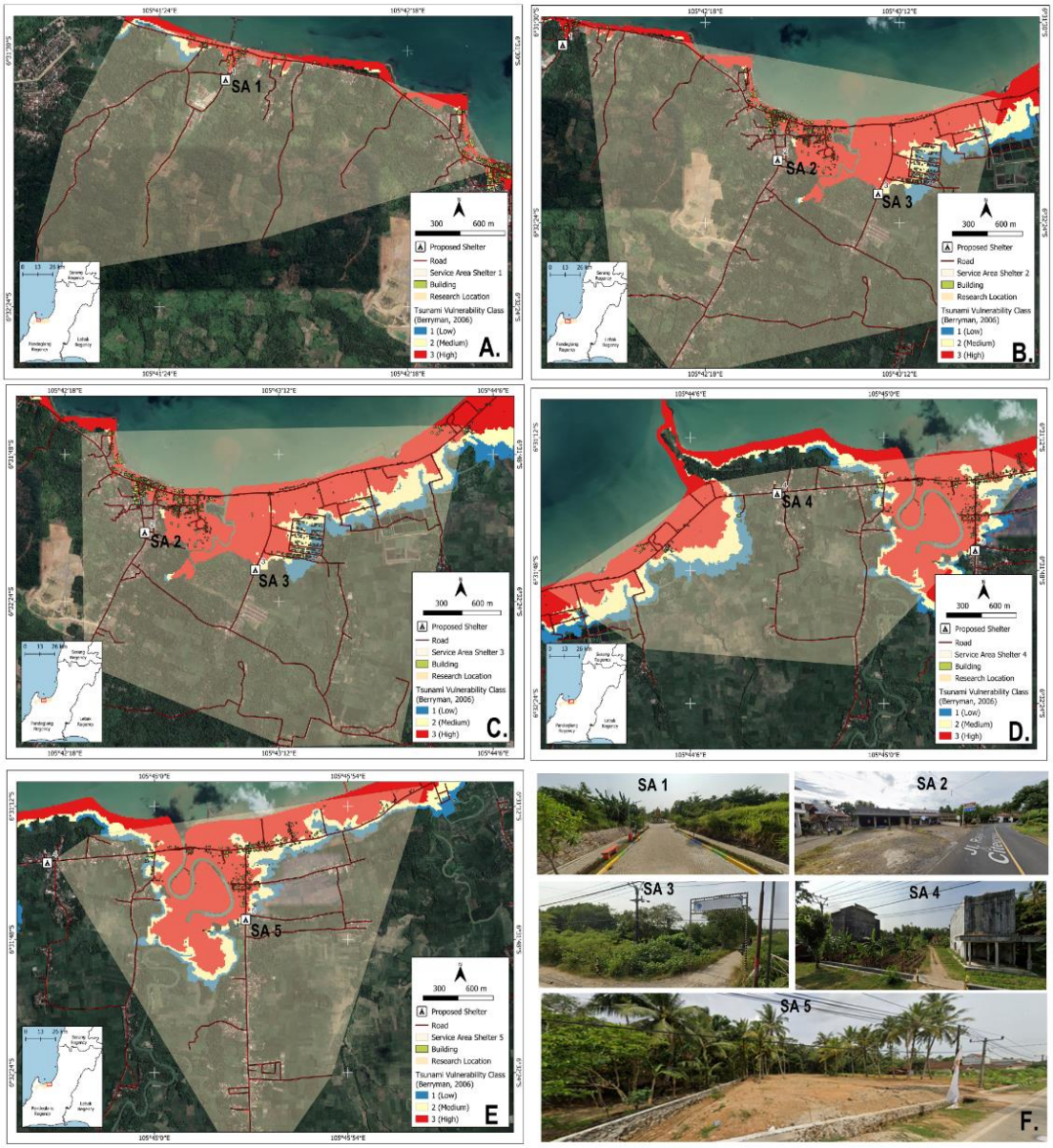

Fig. 5. The service area, proposed as tsunami shelters in the Panimbang Subdistrict; service area 1 (A); service area 2 (B); service area 3 (C); service area 4 (D); service area 5 (E); and the documentation of each shelter (F).

The dense population is observed in the surrounding shelters 2 and 3 (SA2 and SA3), where approximately 6,000 people live. It is situated more than 400 meters from the coastline and on a declivous slope of 4^{o} (**Table 3**). Even though these shelters are sufficiently close to the tsunami inundation zone, they are situated in a higher elevation area (more than 10 meters) (**Figs. 5B** and **5C**). Concerning the service area, these shelters provide the most prominent place amongst the other proposed horizontal TES, with 748.33 and 597.00 ha, respectively.

Shelter 4 (SA4), located in Mekarsari Village, is approximately 400 meters from the coastline with an elevation of 11.93 meters and a slope of 2.48^{o}. This shelter is the closest one to the main road of Panimbang Subdistrict, outside the tsunami inundation zone (**Fig. 5D**). The capacity in this shelter is about 1,584 people, and the service area is 455.47 ha. Therefore, the population density is around

three people per hectare. Unfortunately, compared to the other shelters, this area is the narrowest, with an access width of 2.5 meters and a little offroad. However, land use-wise, the shelter is categorized as an open space (**Table 3**).

The last shelter is SA5, located within Mekarsari Village. It is situated 830 meters from the coastline, with a 9.34 meters elevation and a 0.89^{o} slope (**Fig. 5E** and **Table 3**). This shelter is positioned around 10 meters from the tsunami inundation zone with relatively concrete road materials. It is on the secondary road connecting the Panimbang to Cigeulis Subdistrict, categorized as an open space area. The capacity that could be serviced is approximately 1,440 people within an area of 552.58 ha. Therefore, the population density is two persons per hectare. In addition to the shelter's actual condition, the documentation of every shelter proposed in this study is shown in **Fig. 5F**, where it is generally categorized as an open space area that meets the required criteria for a horizontal tsunami evacuation shelter.

The five proposed horizontal shelters are considered based on the topographical state, accessibility, settlement area's location, open space, and about 200 meters from the coastline. Moreover, these locations were chosen as the safe area based on a 9-meter tsunami simulation. However, different shelter location candidates are possible considering the miscellaneous tsunami properties since there will be a tsunami ranging from 7 to 13.5 meters induced by the Krakatoa eruption in the Sunda Strait, and even a megathrust tsunami may produce a higher run-up propagation (Borrero et al., 2020; Helmi et al., 2020; Ponangsera et al., 2021).

Regarding the service area of shelters, the various shelter area and capacity results in different adaptation for the simulated agents. Several agents are found to evacuate in the other service areas outside their provenance. This decision may also happen during an actual tsunami event. In the ABM simulation, some service areas are overlapping, such as shelters SA2 and SA3, aiming to create a condition where all agents could be accommodated throughout the study area. However, this creates a possibility for agents in these regions to evacuate to nearby shelters where the user has no control over the agent behavior simulated in the model (Almeida et al., 2012; Mas et al., 2012). Since the model considers a coastal topography extracted from DEM data, the inundation pattern seems almost the same with a 9-meter run-up simulation. In this case, the designated shelters are safe from inundation, so the proposed shelters are suitable for mitigating the tsunami impacts when the run-up height is less than 9 meters. More interestingly, a sufficiently high effect is observed in the surrounding estuaries, where estuarine existence and formation could amplify the tsunami run-up in the coastal area (Yeh et al., 2012).

4.3. Results of ABM simulation and estimated casualties

Based on the scenario of five proposed shelters, the ABM was simulated using a NetLogo application to estimate how effective shelter placement is during a tsunami. In this simulation, all evacuees are set to access the shelters on foot at various speeds based on their ages, with a 9-meter tsunami run-up height applied in this scenario. It should be noted that this modeling technique has been tested and used many times by the developer, with, on average, three trials in every single stage (Mas et al., 2015). On the other hand, it is impossible to examine the error of the simulated model when the user cannot look at a piece of code and state that the model has errors (or otherwise) if the programmer's intention is not clearly fathomed and the field data is unavailable (Galán et al., 2009). However, the model certainty was set for a 95% confidence level in this study. Overall, not all evacuees (agents) could be well-evacuated due to several bottleneck blockages (traffic jams) toward the shelter location, resulting in a longer evacuation process.

The ABM was simulated for 50 minutes, whereby the records of agent behavior in every ten minutes are shown in **Fig. 6**, representing the initial collapse due to volcanic-induced tsunami and the ending of the evacuation process done by the simulated agents. The initial condition shown in **Fig. 6A** represents the actual residents' initial location. In this stage, the tsunami commences invading the coastline. After 10 minutes of the simulation, a plethora of agent's movements are observed moving toward the closest proposed shelters. The most observable movements are in the surrounding Ciseukeut estuary (closer to shelter SA5) and shelters 2 and 3 (SA2 and SA3) (**Fig. 6B**).

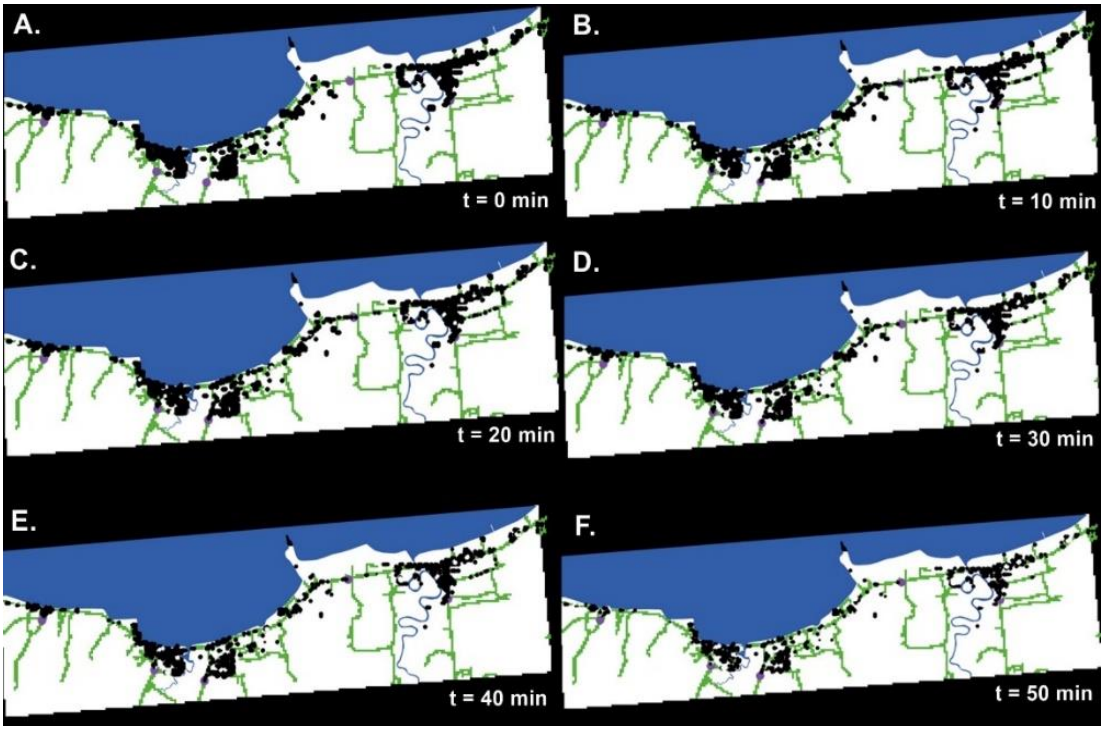

Fig. 6. Agent behavior overview in the study area at different simulation times, t = 0 (A), t = 10 (B), t = 20 (C), t = 30 (D), t = 40 (E), and t = 50 (F) minutes. Black circles denote the simulated agents and purple circles denote the designated shelters.

The number of agents gradually decreases since many of them are evacuated to the nearest proposed shelters. In the time span between 20−30 minutes (**Figs. 6C** and **D**) when the wave height toward the shelters is about 5−6 meters, casualties probably commence to occur where several agents are trapped due to the overcapacity of the primary road towards the shelters. At the 40-minute of the simulation, the total casualties increase, and the inundation level reaches less than three meters towards the shelters (see in **Fig. 6E**).

Generally, the agents will preferably choose the primary roads where several bottleneck blockades are observed in several proposed shelters. At the end of simulation (t = 50 minutes) (**Fig. 6F**), it shows the remnant of agents that fail to evacuate, wherein at some points, there are several agents that do not move anywhere, particularly in the unimpacted areas. More interestingly, due to the crowd passing the primary road toward shelters SA2, SA3, and SA5, the number of casualties is sufficiently high on these shelters.

Of a total of 9,640 agents (people) simulated in the NetLogo, 77.7% are evacuated into the five shelters, and the remnant 22.3% fail to reach the shelters. The highest evacuated agents are observed at shelters SA2 and SA5 (more than 2,000 agents). In contrast, at shelters SA1 and SA4, evacuated agents are under 900. Furthermore, at SA3, around one-third of the total evacuated agent is observed (**Fig. 7**). Concerning the capacity of each shelter, we found that overcapacity shelters are observed at shelters SA1 and SA5, with 12.23% and 59.44%, respectively. By contrast, the other shelters are under the maximum capacity of approximately 40% (**Fig. 7**).

The overcapacity observed at shelters SA1 and SA5 (**Fig. 7**) is unpredictable because it was only considered the denser area with plenty of buildings and settlements as shelters. However, there is no control over agents' fate and response during a tsunami event; this is the limitation of the ABM simulation in this study. This state indicates that shelters SA1 and SA5 cannot accommodate too many evacuees if the tsunami occurs.

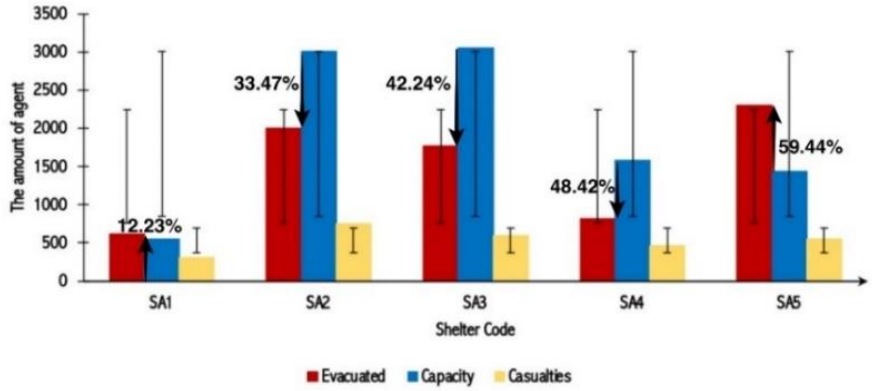

Fig. 7. The estimated amount of evacuated people in every shelter resulted from the ABM modeling. The upward arrows show the shelter's overcapacity condition, and the downward arrows show the shelter's under-capacity condition. Black lines denote the standard deviation of each data.

Regarding the unexpected agent's behavior, they might confuse about where to evacuate during a tsunami invasion, resulting in overcapacity in several shelters (Pamukcu et al., 2020). According to Mas et al. (2012), the ABM simulation could study individual behavior in a complex process of a tsunami. The overcapacity risk condition may occur at shelters SA1 and SA5 if applied in the actual tsunami situation. Therefore, reconsidering these two areas for horizontal evacuation shelters is recommended for further studies whereby the additional shelters in the surrounding areas, perhaps, can avoid the overcapacity conditions.

Regarding the casualties in this simulation, 2,622 agents could not reach the proposed shelters. The highest losses are observed at shelter SA2, with 28% of the total unsafe agents. By contrast, the lowest value is found in the surrounding shelter SA1, with 11% of the total casualties. The other shelters show an almost similar trend, with the losses of approximately 500 agents (**Fig. 7**).

Based on the age classification, the adult category is the most evacuated group, with 3,771 agents compared to the other cohorts (kids, teens, and elders), that only cover around one-third of the highest amount (**Fig. 8**). The exact number of casualties is also observed based on ages ranging from 289 to 1,051 agents. Therefore, most of the residents of Panimbang Subdistrict are categorized as adults (20−64 years old) that can reach the shelter on time. By contrast, the other categories are slower to reach shelters during a tsunami situation.

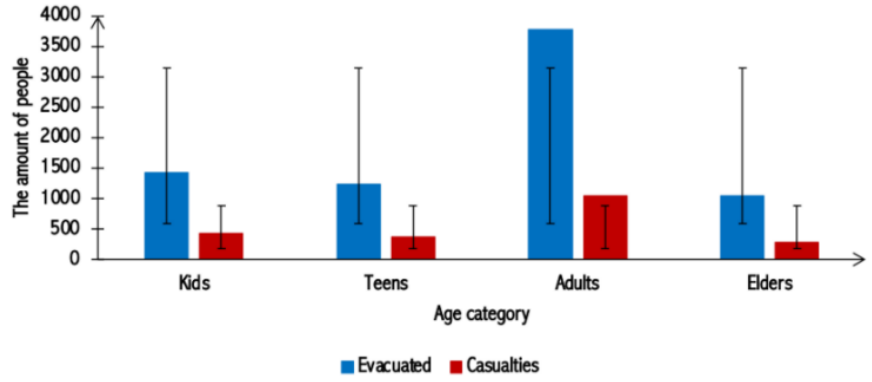

Fig. 8. The estimated amount of evacuated agent and casualties according to the age category. Black lines denote the standard deviation of each data.

In addition to the road accessibility, a "bottleneck" situation is observed, where in the densely populated area, the blocked and collided agents caused by the narrowed road/access are possible (such as at shelters SA2, SA3, and SA4), even though the shelter area and capacity are adequate (Ogawa et al., 2019). That is why the number of casualties simulated via ABM is sufficiently high in these shelters, commonly predominated by the adult category (**Figs. 7** and **8**). However, the study area's demography, the evacuation time, and the evacuee's walking speed also play a significant role in determining the casualties (Ito et al., 2021; Mas et al., 2012). The high value of casualties in this simulation is due to road accessibility, where there is only one main road and some secondary offroad tracks to access the shelters. On the other hand, the model limitation that did not consider the queue toward the proposed shelters and the inability of the agent to reach the shelters also triggers the high number of casualties. This condition may occur during the actual tsunami because of the stressful environment and the effort to survive the tsunami invading the coastal areas (Bakar et al., 2016).

6. CONCLUSIONS

The coastal area of the Panimbang Subdistrict is predominated by highly vulnerable classification based on a 9-meter tsunami inundation modeling. The higher impacted area is observed in the Mekarsari Village than in Citeureup. The highly vulnerable zone to tsunamis is commonly covered by buildings, settlements, and agricultural areas with a declivous slope and low elevation. The extensive tsunami run-up propagation is observed in the riverine and estuarine systems where the dense population does exist, thereby increasing the risk of tsunami-invading rivers.

The five proposed service areas in the Panimbang Subdistrict have met the required criteria for a horizontal evacuation shelter. However, two shelters are reported exceeding the capacity due to the overlapping service area and the limitation of the agent-based modeling used in this study. Moreover, the individual behavior during a complex tsunami process could be studied. Reconsidering the overcapacity shelters by adding several other shelters in the surrounding areas nearby is possible for future studies.

Most evacuees and casualties are of adult age, representing the dominant population of the Panimbang Subdistrict. However, the exact demographic data are essential to estimate the number of evacuees and casualties in the ABM simulation. On the other hand, the sufficiently high casualties are due to the accessibility-induced bottleneck situation whereby the narrowed settlement-shelter connecting road could not accommodate the agents. Furthermore, the simulation did not consider the queue and the inability of agents to reach the designated shelters.

AUTHOR CONTRIBUTIONS

Dini PURBANI, Marza Ihsan MARZUKI, Budianto ONTOWIRJO, Farhan Makarim ZEIN, Didik Wahju Hendro TJAHJO, Sri Endah PURNAMANINGTYAS, Rudhy AKHWADY, and Ulung Jantama WISHA are considered as the main contributors of this article. All authors have read and agreed to the published version of the manuscript.

ACKNOWLEDGMENT

We would like to thank the head of the Research Center for Conservation of Marine and Inland Water Resources, National Research and Innovation Agency (BRIN), Arif Wibowo. Gratitude is also given to those who have helped with the completion of this article.

REFERENCES

Ai, F., Comfort, L. K., Dong, Y., & Znati, T. (2016) A dynamic decision support system based on geographical information and mobile social networks: A model for tsunami risk mitigation in Padang, Indonesia. *Safety Science*, 90. https://doi.org/10.1016/j.ssci.2015.09.022

Almeida, J. E., Kokkinogenis, Z., & Rossetti, R. J. F. (2012) NetLogo implementation of an evacuation scenario. Iberian Conference on Information Systems and Technologies, CISTI.

Bakar, J. A. A., Mat, R. C., Aziz, A. A., Jasri, N. A. N., & Yusoff, M. F. (2016) Designing agent-based modeling in dynamic crowd simulation for stressful environment. *Journal of Telecommunication, Electronic and Computer Engineering*, 8(10).

Berryman, K. (2006) Review of Tsunami Hazard and Risk in New Zealand. In Institute of Geological and Nuclear Sciences (Issue September).

Borrero, J. C., Solihuddin, T., Fritz, H. M., Lynett, P. J., Prasetya, G. S., Skanavis, V., Husrin, S., Kushendratno, Kongko, W., Istiyanto, D. C., Daulat, A., Purbani, D., Salim, H. L., Hidayat, R., Asvaliantina, V., Usman, M., Kodijat, A., Son, S., & Synolakis, C. E. (2020) Field Survey and Numerical Modelling of the December 22, 2018 Anak Krakatau Tsunami. *Pure and Applied Geophysics*, 177(6), 2457‑2475. https://doi.org/10.1007/s00024-020-02515-y

Bricker, J. D., Gibson, S., Takagi, H., & Imamura, F. (2015) On the need for larger Manning's roughness coefficients in depth-integrated tsunami inundation models. *Coastal Engineering Journal*, 57(2). https://doi.org/10.1142/S0578563415500059

Brovelli, M. A., & Zamboni, G. (2018) A new method for the assessment of spatial accuracy and completeness of OpenStreetMap building footprints. *ISPRS International Journal of Geo-Information*, 7(8), 289. https://doi.org/10.3390/ijgi7080289

Danardono, D., Wibowo, A. A., Sari, D. N., Priyono, K. D., & Dewi, E. S. M. (2023) Tsunami Hazard Mapping Based on Coastal System Analysis Using High-Resolution Unmanned Aerial Vehicle (UAV) Imagery (Case Study in Kukup Coastal Area, Gunungkidul Regency, Indonesia). *Geographia Technica*, 18(2), 51-67. http://dx.doi.org/10.21163/GT_2023.182.04

Dogan, G. G., Annunziato, A., Hidayat, R., Husrin, S., Prasetya, G., Kongko, W., Zaytsev, A., Pelinovsky, E., Imamura, F., & Yalciner, A. C. (2021) Numerical Simulations of December 22, 2018 Anak Krakatau Tsunami and Examination of Possible Submarine Landslide Scenarios. *Pure and Applied Geophysics*, 178(1), 1‑20. https://doi.org/10.1007/s00024-020-02641-7

Farahdita, W. L., & Siagian, H. S. R. (2020) Analysis of the area affected by the tsunami in Pandeglang, Banten: A case study of the Sunda Strait Tsunami, in proceedings of IOP Conference Series: Earth and Environmental Science, 429(1). https://doi.org/10.1088/1755-1315/429/1/012052

Galán, J. M., Izquierdo, L. R., Izquierdo, S. S., Santos, J. I., Del Olmo, R., López-Paredes, A., & Edmonds, B. M. (2009) Errors and artefacts in agent-based modelling. *Journal of Artificial Societies and Social Simulation*, 12(1), 1-1.

Grilli, S. T., Tappin, D. R., Carey, S., Watt, S. F. L., Ward, S. N., Grilli, A. R., Engwell, S. L., Zhang, C., Kirby, J. T., Schambach, L., & Muin, M. (2019) Modelling of the tsunami from the December 22, 2018 lateral collapse of Anak Krakatau volcano in the Sunda Straits, Indonesia. *Scientific Reports*, 9(1). https://doi.org/10.1038/s41598-019-48327-6

Helmi, M., Pholandani, Y. H., Setiyono, H., Wirasatriya, A., Atmodjo, W., Widyaratih, R., & Suryoputro, A. A. D. (2020) Intergrated approach of tsunami vulnerability assessment at coastal area of kalianda sub district, south lampung district, lampung Province, Indonesia. *International Journal of Scientific and Technology Research*, 9(3), 1803‑1808.

Husrin, S., Novianto, D., Bramawanto, R., Setiawan, A., Nugroho, D., Permana, S. M., Sufyan, A., Sarnanda, S., Sianturi, D. S. A., Mulyadi, U., Daniel, D., Suhelmi, I. R., & Purnama, M. S. B. (2021). Analisa Kinerja IDSL/PUMMA untuk Peringatan Dini Tsunami di Pangandaran. Jurnal Kelautan Nasional, 16(2). https://doi.org/10.15578/jkn.v16i2.9846

Ito, E., Kosaka, T., Hatayama, M., Urra, L., Mas, E., & Koshimura, S. (2021) Method to extract difficult-to-evacuate areas by using tsunami evacuation simulation and numerical analysis. *International Journal of Disaster Risk Reduction*, 64(102486). https://doi.org/10.1016/j.ijdrr.2021.102486

Jacob, S., Aguilar, L., Wijerathne, L., Hori, M., Ichimura, T., & Tanaka, S. (2014) Agent Based Modeling and Simulation of Tsunami Triggered Mass Evacuation Considering Changes of Environment Due to

Earthquake and Inundation. *Journal of Japan Society of Civil Engineers, Ser. A2 (Applied Mechanics (AM)*, 70(2), 671‑680. https://doi.org/10.2208/jscejam.70.i_671

Kim, K., Kaviari, F., Pant, P., & Yamashita, E. (2022) An agent-based model of short-notice tsunami evacuation in Waikiki, Hawaii. *Transportation Research Part D: Transport and Environment*, 105. https://doi.org/10.1016/j.trd.2022.103239

Kuller, M., Bach, P. M., Roberts, S., Browne, D., & Deletic, A. (2019) A planning-support tool for spatial suitability assessment of green urban stormwater infrastructure. *Science of the Total Environment*, 686, 856‑868. https://doi.org/10.1016/j.scitotenv.2019.06.051

Kurniawan, W., Daryono, Kerta, I., Pranata, B., & Winugroho, T. (2021) Monitoring and analysis of seismic data during the 2018 sunda strait tsunami, in proceedings of E3S Web of Conferences, 331. https://doi.org/10.1051/e3sconf/202133107006

Lakshay, -, Agarwal, A., & Bolia, N. B. (2016) Route Guidance Map for Emergency Evacuation. *Journal of Risk Analysis and Crisis Response*, 6(3), 135‑144. https://doi.org/10.2991/jrarc.2016.6.3.3

Lee, H. S., Sambuaga, R. D., & Flores, C. (2022) Effects of Tsunami Shelters in Pandeglang, Banten, Indonesia, Based on Agent-Based Modelling: A Case Study of the 2018 Anak Krakatoa Volcanic Tsunami. *Journal of Marine Science and Engineering*, 10(8), 1055. https://doi.org/10.3390/jmse10081055

Li, X., Zhang, C., & Li, W. (2017) Building block level urban land-use information retrieval based on Google Street View images. *GIScience and Remote Sensing*, 54(6), 819‑835. https://doi.org/10.1080/15481603.2017.1338389

Marzuki, M. I., Rahmania, R., Kusumaningrum, P. D., Akhwady, R., Sianturi, D. S. A., Firdaus, Y., Sufyan, A., Hatori, C.A. & Chandra, H. (2021) Fishing boat detection using Sentinel-1 validated with VIIRS Data, in Proceedings of IOP Conference Series: Earth and Environmental Science (Vol. 925, No. 1, p. 012058). IOP Publishing.

Mas, E., Koshimura, S., Imamura, F., Suppasri, A., Muhari, A., & Adriano, B. (2015) Recent Advances in Agent-Based Tsunami Evacuation Simulations: Case Studies in Indonesia, Thailand, Japan and Peru. *Pure and Applied Geophysics*, 172(12), 3409‑3424. https://doi.org/10.1007/s00024-015-1105-y

Mas, E., Suppasri, A., Imamura, F., & Koshimura, S. (2012) Agent-based Simulation of the 2011 Great East Japan Earthquake/Tsunami Evacuation: An Integrated Model of Tsunami Inundation and Evacuation. *Journal of Natural Disaster Science*, 34(1), 41‑57. https://doi.org/10.2328/jnds.34.41

Mostafizi, A., Wang, H., Cox, D., Cramer, L. A., & Dong, S. (2017) Agent-based tsunami evacuation modeling of unplanned network disruptions for evidence-driven resource allocation and retrofitting strategies. *Natural Hazards*, 88(3), 1347‑1372. https://doi.org/10.1007/s11069-017-2927-y

Mück, M., & Post, D. J. (2008). Mück, M., & Post, D. J. (2008) Tsunami Evacuation Modelling. Development and application of a spatial information system supporting tsunami evacuation planning in South-West Bali (Vol. 131). Institut für Geographie Universität Regensburg.

Muhari, A., Heidarzadeh, M., Susmoro, H., Nugroho, H. D., Kriswati, E., Supartoyo, Wijanarto, A. B., Imamura, F., & Arikawa, T. (2019) The December 2018 Anak Krakatau Volcano Tsunami as Inferred from Post-Tsunami Field Surveys and Spectral Analysis. *Pure and Applied Geophysics*, 176(12), 5219‑5233. https://doi.org/10.1007/s00024-019-02358-2

Mulyadi, D., & Nur, W. H. (2018) The Analytic Hierarchy Process Application for EarthQuacke Hazard in Tanjung Lesung-Panimbang Pandeglang. *RISET Geologi Dan Pertambangan*, 28(1), 37‑48. https://doi.org/10.14203/risetgeotam2018.v28.387

Naser, M., & Birst, S. C. (2010) Mesoscopic evacuation modeling for small to medium size metropolitan areas.

Ogawa, Y., Akiyama, Y., Yokomatsu, M., Sekimoto, Y., & Shibasaki, R. (2019). Estimation of supply chain network disruption of companies across the country affected by the Nankai trough earthquake Tsunami in Kochi city. *Journal of Disaster Research*, 14(3), 508‑520. https://doi.org/10.20965/jdr.2019.p0508

Pamukcu, D., Zobel, C. W., & Arnette, A. (2020) Characterizing social community structures in emergency shelter planning, In Proceedings of the International ISCRAM Conference, 2020-May.

Paris, R., Switzer, A. D., Belousova, M., Belousov, A., Ontowirjo, B., Whelley, P. L., & Ulvrova, M. (2014) Volcanic tsunami: A review of source mechanisms, past events and hazards in Southeast Asia (Indonesia, Philippines, Papua New Guinea). *Natural Hazards*, 70(1), 447‑470. https://doi.org/10.1007/s11069-013-0822-8

Pesaresi, M., Corbane, C., Julea, A., Florczyk, A. J., Syrris, V., & Soille, P. (2016) Assessment of the added-value of Sentinel-2 for detecting built-up areas. *Remote Sensing*, 8(4), 299. https://doi.org/10.3390/rs8040299

Phiri, D., Simwanda, M., Salekin, S., Nyirenda, V. R., Murayama, Y., & Ranagalage, M. (2020) Sentinel-2 data for land cover/use mapping: A review. *Remote Sensing*, 12, (14). https://doi.org/10.3390/rs12142291

Pizarro, V., Leger, P., Hidalgo-Alcázar, C., & Figueroa, I. (2022) ABM RoutePlanner: An agent-based model simulation for suggesting preference-based routes in Spain. *Journal of Simulation*. https://doi.org/10.1080/17477778.2022.2027826

Ponangsera, I. S., Kurniadi, A., Ayu Puspitosari, D., & Hartono, D. (2021) Determination of tsunami run-up and golden time in the megathrust subduction zone of the sunda strait segment, in proceedings of E3S Web of Conferences, 331. https://doi.org/10.1051/e3sconf/202133107007

Pradjoko, E., Kusuma, T., Setyandito, O., Suroso, A., & Harianto, B. (2015) The Tsunami Run-up Assesment of 1977 Sumba Earthquake in Kuta, Center of Lombok, Indonesia. *Procedia Earth and Planetary Science*, 14, 9–16. https://doi.org/10.1016/j.proeps.2015.07.079

Priohutomo, K., Nugroho, W. H., Arianti, E., & Priatno, D. H. (2022) Fatigue Life Prediction of Mooring Line on Indonesian Tsunami Early Warning Systems (Ina-TEWS) Buoy, in proceedings of IOP Conference Series: Earth and Environmental Science, 972(1). https://doi.org/10.1088/1755-1315/972/1/012011

Sahal, A., Leone, F., & Péroche, M. (2013) Complementary methods to plan pedestrian evacuation of the French Riviera's beaches in case of tsunami threat: Graph-and multi-agent-based modelling. *Natural Hazards and Earth System Sciences*, 13(7). https://doi.org/10.5194/nhess-13-1735-2013

Sari, D. A. P., & Soesilo, T. E. B. (2020) Measuring Community Resilience to the Tsunami Disaster (Study of Sukarame Village, Carita District, Pandeglang Regency). In proceedings of IOP Conference Series: Earth and Environmental Science, 448(1). https://doi.org/10.1088/1755-1315/448/1/012092

Taubenböck, H., Goseberg, N., Lämmel, G., Setiadi, N., Schlurmann, T., Nagel, K., Siegert, F., Birkmann, J., Traub, K.-P., Dech, S., Keuck, V., Lehmann, F., Strunz, G., & Klüpfel, H. (2013) Risk reduction at the "Last-Mile": an attempt to turn science into action by the example of Padang, Indonesia. *Natural Hazards*, 65(1), 915–945. https://doi.org/10.1007/s11069-012-0377-0

Triyono, R., Prasetya, T., Daryono, D., Anugrah, S. D., Sudrajat, A., Setiyono, U., Gunawan, I., Priyobudi, P., Yatimantoro, T., Hidayanti, H., Anggraini, S., Rahayu, R. H., Yogaswara, D. S., Hawati, P., Apriani, M., Julius, A. M., Harvan, M., Simangunsong, G., & Kriswinarso, T. (2019) Katalog Tsunami Indonesia Tahun 416-2018 (M. Sadly (ed.); 1st ed.). Badan Meteorologi dan Geofisika (BMKG). (In Indonesian).

Usman, F., Murakami, K., Dwi Wicaksono, A., & Setiawan, E. (2017) Application of Agent-Based Model Simulation for Tsunami Evacuation in Pacitan, Indonesia, in proceedings of MATEC Web of Conferences, 97. https://doi.org/10.1051/matecconf/20179701064

Vargas-Munoz, J. E., Srivastava, S., Tuia, D., & Falcao, A. X. (2021) OpenStreetMap: Challenges and Opportunities in Machine Learning and Remote Sensing. *IEEE Geoscience and Remote Sensing Magazine*, 9(1). https://doi.org/10.1109/MGRS.2020.2994107

Wafda, F., Saputra, R. W., Nurdin, Y., Nasaruddin, & Munadi, K. (2013) Agent-based tsunami evacuation simulation for disaster education, in proceedings of International Conference on ICT for Smart Society 2013: "Think Ecosystem Act Convergence", ICISS 2013. https://doi.org/10.1109/ICTSS.2013.6588087

Wang, Z., & Jia, G. (2021) A novel agent-based model for tsunami evacuation simulation and risk assessment. *Natural Hazards*, 105(2), 2045–2071. https://doi.org/10.1007/s11069-020-04389-8

Wang, Z., & Jia, G. (2022) Simulation-Based and Risk-Informed Assessment of the Effectiveness of Tsunami Evacuation Routes Using Agent-Based Modeling: A Case Study of Seaside, Oregon. *International Journal of Disaster Risk Science*, 13(1). https://doi.org/10.1007/s13753-021-00387-x

Yamanaka, Y., & Shimozono, T. (2022) Tsunami inundation characteristics along the Japan Sea coastline: effect of dunes, breakwaters, and rivers. *Earth, Planets and Space*, 74(1). https://doi.org/10.1186/s40623-022-01579-5

Yeh, H., Tolkova, E., Jay, D., Talke, S., & Fritz, H. (2012) Tsunami hydrodynamics in the Columbia River. *Journal of Disaster Research*, 7(5), 604–608. https://doi.org/10.20965/jdr.2012.p0604

Zaman, M. B., Kobayashi, E., Wakabayashi, N., Khanfir, S., Pitana, T., & Maimun, A. (2014) Fuzzy FMEA model for risk evaluation of ship collisions in the Malacca Strait: Based on AIS data. *Journal of Simulation*, 8(1). https://doi.org/10.1057/jos.2013.9